Bol. Soc. Paran. Mat.
©SPM –ISSN-2175-1188 on line
SPM: www.spm.uem.br/bspm

(3s.) **v. 2024 (42)** : 1–12.
ISSN-0037-8712 in press
doi:10.5269/bspm.63895

A Class of Central Unstaggered Schemes for Nonlocal Conservation Laws: Applications to Traffic Flow Models

Said Belkadi and Mohamed Atounti

ABSTRACT: This study introduces a new class of central unstaggered finite volume methods for approximating solutions to nonlocal conservation laws. The proposed method is based on Nessyahu and Tadmor's (NT). Instead of solving Riemann's problems at the level of cell interfaces, as in the NT scheme, the approach we develop implicitly uses ghost cells while still generating the numerical solution on a single grid. We use our method with the aim of solving one-dimensional, nonlocal traffic flow problems. The numerical results we present demonstrate the accuracy, high resolution, and non-oscillatory nature of the proposed method and compare very favorably with those obtained using the original NT method, demonstrating the expected simplicity of a family of unstaggered central schemes and confirming that nonlocal traffic flow models can be treated very efficiently by the suggested method.

Key Words: Scalar conservation laws, non-local flux, traffic flow model, finite volume schemes.

Contents

1. Introduction

The second-order, non-oscillatory central scheme was introduced in the early 1990s by Nessyahu and Tadmor in [19]. The NT scheme is a first-order staggered Lax-Friedrich extension that evolves numerical solutions on an original grid and a staggered dual grid over time steps. The NT method is second-order accurate due to a piecewise linear numerical solution constructed on the cells. In the NT method, slope limiting is also used to prevent oscillations in the numerical solution.

Recently, non-oscillatory NT-type central schemes [12,17] have been proposed for solving nonlocal conservation laws. These NT-type schemes have been used successfully to solve problems in traffic flow models [5,16], and sedimentation models [4,7]. Besides, other nonlocal traffic flow models have also been proposed and investigated in [2,3,8,9,11,15,18,19,20].

The fact that the numerical solution in NT-type schemes requires two grids at successive time steps, on the other hand, is considered as a flaw in the method [23]. To put it more specifically, a synchronization problem develops if the numerical solution calculated using an NT-type base scheme needs additional processing to retain a physical property. This is since each continuation of the updated solution needs the solution values calculated at various times. The problem gets harder when the original and dual-staggered cells don't have the same sizes.

2010 *Mathematics Subject Classification:* 35L65, 90B20, 65M08, 65M12
Submitted August 01, 2022. Published January 14, 2023

In [14], Jiang et al. provided an unstaggered adaptation of the NT scheme; the method they created incorporates the Nessyahu and Tadmor iteration formulas, but the second iteration contains a zero-time step. In [22], R.Touma developed a one-dimensional unstaggered central scheme for shallow water equations and later derived the same solution for hyperbolic systems [23]. He described a method that can be considered an unstaggered adaption of the NT scheme and a generalization of the technique presented in [14].

This study develops a class of second-order accurate unstaggered central schemes (UCS) to solve the nonlocal conservation laws arising in traffic flow models. The approach that we suggest is a two-parameter method in one spatial dimension; it is a generalization of the method presented in [23], which is Riemann problem solverfree and pertinent to the traffic flow model investigated in this work. It is built on a single grid. However, it employs ghost staggered cells to avoid Riemann problem resolution at cell interfaces. As a result, the central scheme is second-order accurate and unstaggered. The numerical results produced by the UCS method in Section 4 conform with the results obtained by the NT original, demonstrating the suggested method's efficiency, robustness, high resolution, and simplicity.

The present work is structured as follows: In Section 2, we present a one-dimensional nonlocal traffic flow model. We start in Section 3 with a brief overview of Nessyahu-Tadmor schemes (NT) for nonlocal conservation laws, and we proceed to construct our new unstaggered central scheme. In Section 4, we offer a number of numerical tests. We end by giving the conclusion in Section 5.

2. Non-local traffic flow model.

We propose the following one-dimensional traffic flow with a nonlocal mean velocity [12]:

$$\partial_t \rho + \partial_x \left(g(\rho) v \left(\kappa_\eta * \rho(t,x) \right) \right) = 0, \ x \in \mathbb{R}, \ t > 0, \tag{2.1}$$

with

$$\kappa_\eta * \rho(t,x) = \int_x^\infty \kappa_\eta(y-x)\rho(t,y)dy), \ x \in \mathbb{R}, \ t > 0, \tag{2.2}$$

ρ represents vehicle density, v represents mean velocity, and κ_η is a kernel function whose support is proportional to drivers' look-ahead distance, which must be adjusted to the average downstream traffic density. The model (2.1) is a nonlocal version of the Lighthill-Whitham-Richards (LWR) model [5]. It reflects drivers' behavior in reacting to events in front of them and adjusting their speed when considering downstream density. Assume $\rho \in [0, \rho_{\max}]$, $v(0) = v_{\max}$, and $v(\rho_{\max}) = 0$ ($\rho_{\max}$ is the maximum velocity).

For a well-posed model in the following section, we put forward the following assumptions on the velocity function v, the function g and the kernel function κ_η (see, [1,12]):

$$\begin{array}{ll} g \in C^1\left([0,\rho_{max}],\mathbb{R}\right), & \\ \kappa_\eta \in C^2\left([0,\eta],\mathbb{R}^+\right), & \kappa_\eta^{'} \leqslant 0, \ \int_0^\eta \kappa_\eta(x)dx = 1 \\ v \in C^2([0,\rho_{max}],\mathbb{R}^+), & v' \leqslant 0. \end{array} \tag{2.3}$$

3. Numerical scheme.

This section aims to give a brief overview of the Nessyahu–Tadmor scheme and then construct our new central unstaggered numerical scheme to solve nonlocal conservation laws.

3.1. Nessyahu–Tadmor central scheme: brief overview

We consider the initial value problem:

$$\begin{cases} \partial_t \rho + \partial_x F\left(\rho, U\right) = 0, & x \in \mathbb{R}, \ t > 0, \\ \rho(0,x) = \rho_0(x), & \rho_0 \in BV\left(\mathbb{R}, [0,\rho_{max}]\right), \end{cases} \tag{3.1}$$

where U denote the downstream convolution product as

$$U = \kappa_\eta * \rho.$$

and

$$F(\rho, U) = g(\rho)v(U).$$

Here, BV denotes the space of functions with bounded variation, i.e.

$$\mathrm{BV} = \{u \in L^1(\mathbb{R})/\mathrm{TV}(u) < \infty\}, \text{ with } \mathrm{TV}(u) = \sup_{\varepsilon>0} \frac{1}{\varepsilon} \int_{\mathbb{R}} |u(x+\varepsilon) - u(x)|dx.$$

We first split the computational domain into uniform cells. $C_j = [x_{j-\frac{1}{2}}; x_{j+\frac{1}{2}}]$ of length Δx, where $x_{j+\frac{1}{2}} = (j+\frac{1}{2})\Delta x$ are the cell interfaces and $x_j = j\Delta x$ are the cell centers.

The computed solution is realized in terms of its cell averages, as with all finite-volume methods [10,13]

$$\rho_j^n = \frac{1}{\Delta x} \int_{x_{j-\frac{1}{2}}}^{x_{j+\frac{1}{2}}} \rho(t^n, x)dx. \tag{3.2}$$

They are assumed to be known at a given time t^n, and are then evolved through time using the explicit conservative formula below:

$$\frac{\rho_j^{n+1} - \rho_j^n}{\Delta t} = \frac{F_{j-\frac{1}{2}} - F_{j+\frac{1}{2}}}{\Delta x}, \tag{3.3}$$

where $F_{j\pm\frac{1}{2}}$ is the numerical flux at the interface $x_{j\pm\frac{1}{2}}$.

The NT scheme [19] is based on the staggered Lax-Friedrich method. By alternating the numerical solution on an original and a staggered grid, it avoids solving Riemann issues at cell interfaces. Furthermore, the NT scheme reconstructs the piecewise constant solution obtained at the preceding time-step (3.2) using a piecewise linear reconstruction:

$$\tilde{\rho}^n(x) = \rho_j^n + \sigma_j^n(x - x_j), \qquad x \in C_j, \tag{3.4}$$

where the slope σ_j^n is an approximation to the derivative $\frac{\partial \rho}{\partial x}\rfloor_{x=x_i}$ in the interval C_j. In the following, we will assume that the approximate slopes σ_j satisfy

$$\sigma_j^n \simeq \frac{\partial \rho}{\partial x}\rfloor_{x=x_i} + o(\Delta x),$$

this leads to a numerical solution accurate to the second-order in space. The predictor-corrector time discretization ensures second-order temporal accuracy. On the staggered cells, the solution at time t^{n+1} is computed as follows:

$$\rho_{j+\frac{1}{2}}^{n+1} = \frac{\rho_j^n + \rho_{j+1}^n}{2} + \frac{\Delta x}{8}\left(\sigma_j^n - \sigma_{j+1}^n\right) - \lambda\left(F(\rho_{j+1}^{n+\frac{1}{2}}, U_{j+1}^{n+\frac{1}{2}}) - F(\rho_j^{n+\frac{1}{2}}, U_j^{n+\frac{1}{2}})\right), \quad \lambda = \frac{\Delta t}{\Delta x}. \tag{3.5}$$

The values $\rho_j^{n+\frac{1}{2}}$ and $U_j^{n+\frac{1}{2}}$ are obtained from ρ_j^n and U_j^n respectively by Eqs (3.7), (3.10) described below. We refer to [12] for a complete description of the one-dimensional NT scheme.

3.2. Unstaggered central schemes reconstruction

We shall now design our new central unstaggered numerical scheme while maintaining all the characteristics of the original NT scheme. This new scheme proceeds in two steps. First, we assume the numerical solution for ρ_i^n at time t^n is known, that is,

$$\rho_i^n = \frac{1}{\Delta x} \int_{x_{i-\frac{1}{2}}}^{x_{i+\frac{1}{2}}} \rho(t^n, x)dx. \tag{3.6}$$

We define the ghost staggered cells $G_{i+\frac{1}{2}} = [x_i, x_{i+1}]$ and use Nessyahu and Tadmor's formula (3.5) to get a solution estimate $\rho_{i+\frac{1}{2}}^{n+1}$ at time t^{n+1} on the ghost cells $G_{i+\frac{1}{2}}$ as follows:

$$\rho_{j+\frac{1}{2}}^{n+1} = \frac{\rho_j^n + \rho_{j+1}^n}{2} + \frac{\Delta x}{8}\left(\sigma_j^n - \sigma_{j+1}^n\right) - \lambda\left(F(\rho_{j+1}^{n+\frac{1}{2}}, U_{j+1}^{n+\frac{1}{2}}) - F(\rho_j^{n+\frac{1}{2}}, U_j^{n+\frac{1}{2}})\right). \tag{3.7}$$

In Eq. (3.7), the values $\rho_i^{n+\frac{1}{2}}$ and $U_i^{n+\frac{1}{2}}$ at the intermediate time are estimated values defined by an intermediary predictor step that uses a first-order Taylor expansion and the original equation (3.5) as follows:

$$\rho_j^{n+\frac{1}{2}} = \rho_j^n - \frac{\Delta t}{2}\partial_x F(\rho(t^n, x_j), U(t^n, x_j)), \tag{3.8}$$

$$U_j^{n+\frac{1}{2}} = U_j^n + \frac{\Delta t}{2} U_t(t^n, x_j), \tag{3.9}$$

where the flux derivative $\partial_x F(\rho(t^n, x_j), U(t^n, x_j))$ in Eq. (3.8) and the slope of the reconstruction in Eq. (3.4) are computed with nonlinear limiters needed to ensure the nonoscillatory nature of the reconstruction (3.7). In this work we have used generalized minmod (mm) limiter family [6,21] as follows:

$$\partial_x F(\rho(t^n, x_j), U(t^n, x_j)) = \mathrm{mm}\Bigg(\theta \mathrm{mm}\left(\frac{F(\rho_j^n, U_j^n) - F(\rho_{j-1}^n, U_{j-1}^n)}{\Delta x}, \frac{F(\rho_{j+1}^n, U_{j+1}^n) - F(\rho_j^n, U_j^n)}{\Delta x}\right), \frac{F(\rho_{j+1}^n, U_{j+1}^n) - F(\rho_{j-1}^n, U_{j-1}^n)}{2\Delta x}\Bigg)$$

$$\sigma_j^n = \mathrm{mm}\left(\theta \mathrm{mm}\left(\frac{\rho_j^n - \rho_{j-1}^n}{\Delta x}, \frac{\rho_{j+1}^n - \rho_j^n}{\Delta x}\right), \frac{\rho_{j+1}^n - \rho_{j-1}^n}{2\Delta x}\right),$$

where $\theta \in [1, 2]$ is a parameter and the minmod function is defined by

$$\text{minmod(a,b)} = \begin{cases} \text{sgn(a)}.\min(|a|, |b|) & \text{if } a.b > 0, \\ 0 & \text{otherwise.} \end{cases}$$

In Eq. (3.9), if $\eta = N\Delta x$ for some $N \in \mathbb{N}$, then we can compute the terms by using the mid-point and the composite trapezoidal rules [6] as follows:

$$\begin{aligned} U(t^n, x_j) &= \int_{x_j}^{x_j+\eta} \rho(t^n, y)\, \kappa_\eta(y - x_j)\, dy \\ &\approx \int_{x_j}^{x_{j+\frac{1}{2}}} \tilde{\rho}^n(y)\kappa_\eta(y - x_j)dy + \int_{x_{j+N-\frac{1}{2}}}^{x_{j+N}} \tilde{\rho}^n(y)\kappa_\eta(y - x_j)dy \\ &\quad + \sum_{k=1}^{N-1} \int_{x_{j+k-\frac{1}{2}}}^{x_{j+k+\frac{1}{2}}} \tilde{\rho}^n(y)\kappa_\eta(y - x_j)dy \\ &= \left[\kappa_\eta(0)\rho_j^n + \kappa_\eta(\tfrac{\Delta x}{2})(\rho_j^n + \sigma_j \tfrac{\Delta x}{2})\right] \tfrac{\Delta x}{4} \\ &\quad + \left[\kappa_\eta(x_N)\rho_{j+N}^n + \kappa_\eta(x_{N-\frac{1}{2}})\left(\rho_{j+N}^n - \sigma_{j+N}\tfrac{\Delta x}{2}\right)\right] \tfrac{\Delta x}{4} \\ &\quad + \sum_{k=1}^{N-1} \Delta x \kappa_\eta(k\Delta x)\rho_{j+k}^n, \end{aligned} \tag{3.10}$$

and

$$\begin{aligned} U_t(t^n, x_j) &= \int_{x_j}^{x_j+\eta} \rho_t(t^n, y)\kappa_\eta(y - x_j)dy \\ &= -\int_{x_j}^{x_j+\eta} F_y\left(\rho(t^n, y), U(t^n, y)\right)\kappa_\eta(y - x_j)dy \\ &= -\left[\kappa_\eta\left(y - x_j\right) F\left(\rho\left(t^n, y\right), U(t^n, y)\right)\right]_{x_j}^{x_j+\eta} \\ &\quad + \int_{x_j}^{x_j+\eta} \kappa'_\eta(y - x_j)F\left(\rho(t^n, y), U(t^n, y)\right) dy \qquad (3.11) \\ &= \kappa_\eta\left(0\right) F\left(\rho_j^n, U_j^n\right) - \kappa_\eta\left(x_N\right) F\left(\rho_{j+N}^n, U_{j+N}^n\right) \\ &\quad + \left[\kappa'_\eta(0)F\left(\rho_j^n, U_j^n\right) + \kappa'_\eta\left(\eta\right) F\left(\rho_{j+N}^n, U_{j+N}^n\right)\right] \frac{\Delta x}{2} \\ &\quad + \sum_{k=1}^{N} \Delta x\kappa'_\eta(x_k)F\left(\rho_{j+k}^n, U_{j+k}^n\right). \end{aligned}$$

The second step of the proposed UCS approach is to return the updated solution achieved on the ghost staggered cells to the original grid. We first define the piecewise linear reconstructions of the ghost cell values $\tilde{\rho}_{i+\frac{1}{2}}$ since the numerical solution is defined using piecewise linear reconstructions of the piecewise constant solution defined at the center of the cells C_i and $G_{i+\frac{1}{2}}$.

$$\tilde{\rho}_{i+\frac{1}{2}}(x, t^{n+1}) = \rho_{i+\frac{1}{2}}^{n+1} + \delta_{i+\frac{1}{2}}^{n+1}(x - x_{i+\frac{1}{2}}), \qquad x \in [x_i, x_{i+1}] \tag{3.12}$$

where $\delta_{i+\frac{1}{2}}^{n+1}$ is an approximate slope associated with the piecewise linear reconstruction in the ghost cell $G_{i+\frac{1}{2}}$, it is chosen as:

$$\delta_{i+\frac{1}{2}}^{n+1} = \text{mm}\left(\theta\text{mm}\left(\frac{\rho_{j+\frac{1}{2}}^n - \rho_{j-\frac{1}{2}}^n}{\Delta x}, \frac{\rho_{j+\frac{3}{2}}^n - \rho_{j+\frac{1}{2}}^n}{\Delta x}\right), \frac{\rho_{j+\frac{3}{2}}^n - \rho_{j-\frac{1}{2}}^n}{2\Delta x}\right), \ \theta \in [1, 2], \tag{3.13}$$

we then define the solution values ρ_i^{n+1} at time t^{n+1} as follows:

$$\rho_i^{n+1} = \alpha\tilde{\rho}_{i-\frac{1}{2}}\left(t^{n+1}, (1-\beta)x_{i-\frac{1}{2}} + \beta x_i\right) + (1-\alpha)\tilde{\rho}_{i+\frac{1}{2}}\left(t^{n+1}, (1-\beta)x_{i+\frac{1}{2}} + \beta x_i\right), \ \alpha \in [0, 1], \ \beta \in [0, 1]. \tag{3.14}$$

So with the help of (3.12), Eq. (3.14) is rewritten as

$$\rho_i^{n+1} = \alpha\rho_{i-\frac{1}{2}}^{n+1} + (1-\alpha)\rho_{i+\frac{1}{2}}^{n+1} + \beta\frac{\Delta x}{2}\left(\alpha\delta_{i-\frac{1}{2}}^{n+1} - (1-\alpha)\delta_{i+\frac{1}{2}}^{n+1}\right). \tag{3.15}$$

As we shall see in numerical tests, for all α best results are obtained when $\beta = 0.25$. The resulting scheme is second-order accurate both in time and space and possesses the same stability condition as the original NT. In summary, the utilization of the proposed UCS scheme to approach the solution of nonlocal conservation law (3.1) suggests the following algorithm:

1. Given ρ_j^n for $j \in \mathbb{N}$, approximation of the cell averages of $\rho(t; x)$ at t^n.
2. Compute U_j^n and its derivative U_t^n using (3.10) and (3.11).
3. Compute the staggered cell averages $\rho_{j+\frac{1}{2}}^{n+1}$ at time t^{n+1} on the ghost cells using Eq. (3.7).
4. Compute the solution at time t^{n+1} on the original and unique grid using Eq. (3.15)

4. Numerical Results

In this section, we solve (3.1) numerically within the domain $[0,T]\times[-1;1]$. We illustrate this with several numerical examples. Then we set $f(\rho)=\frac{\rho^2}{2}$ and $v(\rho)=v_{\max}\left(1-\left(\frac{\rho}{\rho_{\max}}\right)^n\right)$ with $n\in\{1,2\}$ (maximum velocity and maximum density equal to 1). Taking hypotheses (2.3) into account, we fix $\eta=0.1$ and choose the kernel function as $\kappa_\eta(x)=\frac{2}{\eta}(1-\frac{x}{\eta})$. In all of the tests, the solution was based on a uniform grid of 400 cells, with a time step determined by

$$\lambda<\frac{1}{2\lambda_{\max}},\quad \lambda_{\max}:=\max_{\rho\in[0,\rho_{\max}]}|\frac{dF(\rho,U)}{d\rho}|.$$

Similar to this, the choice of the limiter in the numerical computation of gradients can have a substantial impact on the quality of the numerical resolution in central schemes as well as other numerical approaches. In this investigation, we chose the generalized minmod limiter with $\theta=2$.

Consider two different initial conditions for the initial value problem (3.1). The first is the smooth function, which is as follows:

$$\rho_0(x)=0.5+0.4\sin(x). \tag{4.1}$$

The discontinuous one is,

$$\rho_0(x)=\begin{cases}0.8, & \text{if } x>0,\\ 0.2, & \text{if } x<0.\end{cases} \tag{4.2}$$

4.1. The efficiency of the UCS

In this subsection, we numerically examine the effectiveness of the suggested approach, by comparing the UCS scheme's solution for a number of various values of the parameters α and β: We fix the parameter α in each of our three tests and compute the solution at time $T=0.5$. We set $\Delta x=0.005$ and compute the solutions using UCS schemes with the following different parameter values $\beta=0.1,0.25,0.5,0.75$. The results are displayed in Figs. 1-6 are compared to a reference solution computed with a UCS scheme and $\Delta x=0.000625$. Compared to the reference solution, we observe that UCS with $\beta=0.25$ is more accurate than others. Also, when $\beta=0.25$, the non-oscillatory nature of our scheme can be seen in all figures.

Test case 1: $\alpha=0.5$

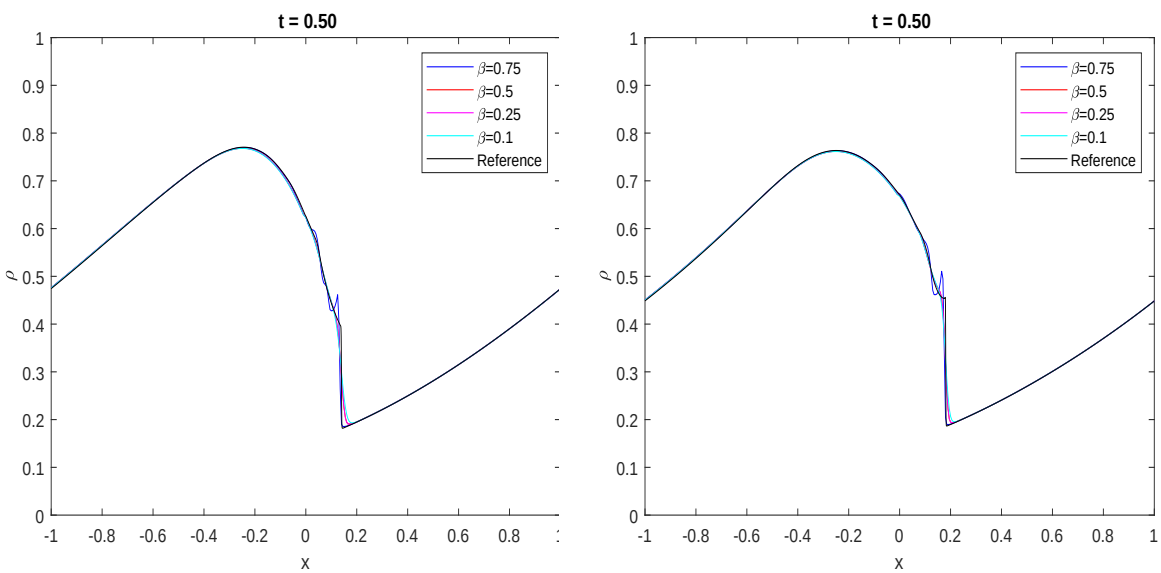

Figure 1: Solutions of (3.1), (4.1) computed by the UCS scheme using, $v(\rho)=1-\rho$(left) and $v(\rho)=1-\rho^2$(right).

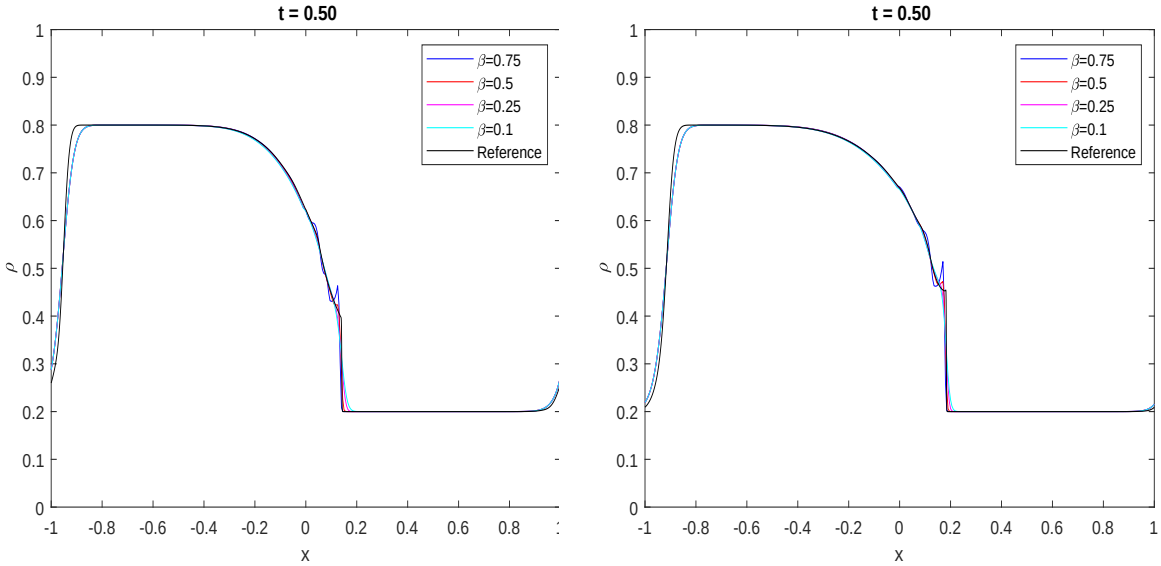

Figure 2: Solutions of (3.1), (4.2) computed by the UCS scheme using $v(\rho) = 1-\rho$ (left) and $v(\rho) = 1-\rho^2$ (right).

Test case 2: $\alpha = 0.25$

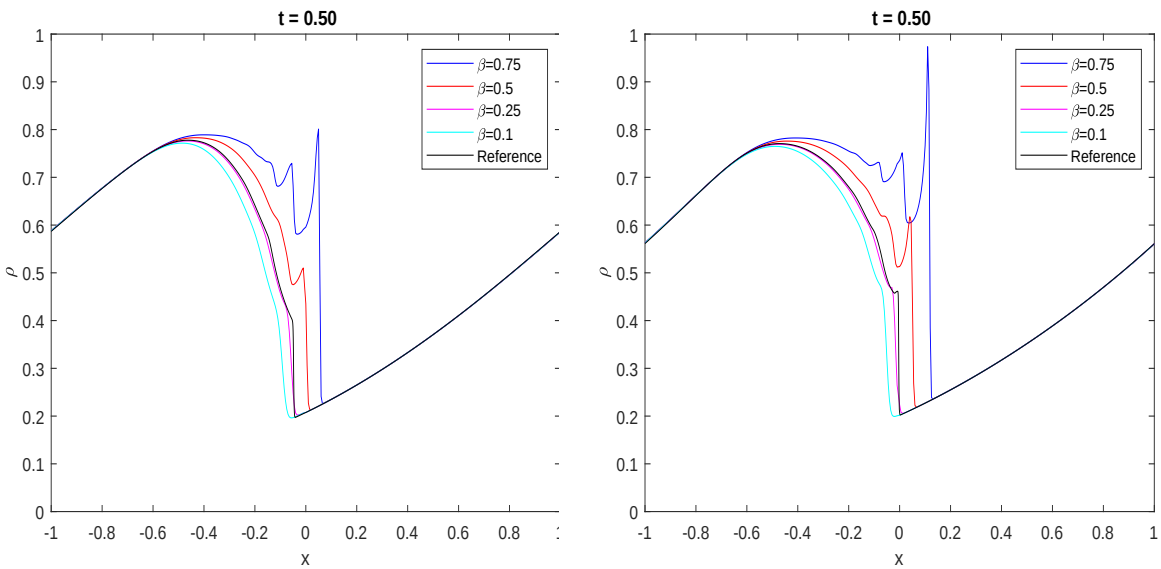

Figure 3: Solutions of (3.1), (4.1) computed by the UCS scheme using $v(\rho) = 1-\rho$ (left) and $v(\rho) = 1-\rho^2$ (right).

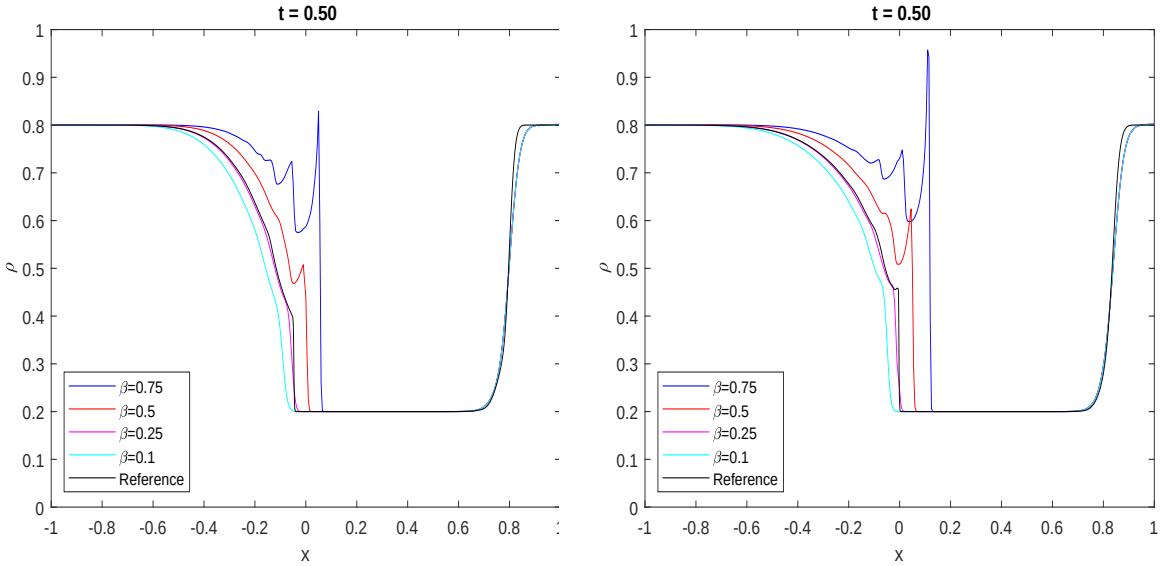

Figure 4: Solutions of (3.1), (4.2) computed by the UCS scheme using $v(\rho) = 1-\rho$ (left) and $v(\rho) = 1-\rho^2$ (right).

Test case 3: $\alpha = 0.75$

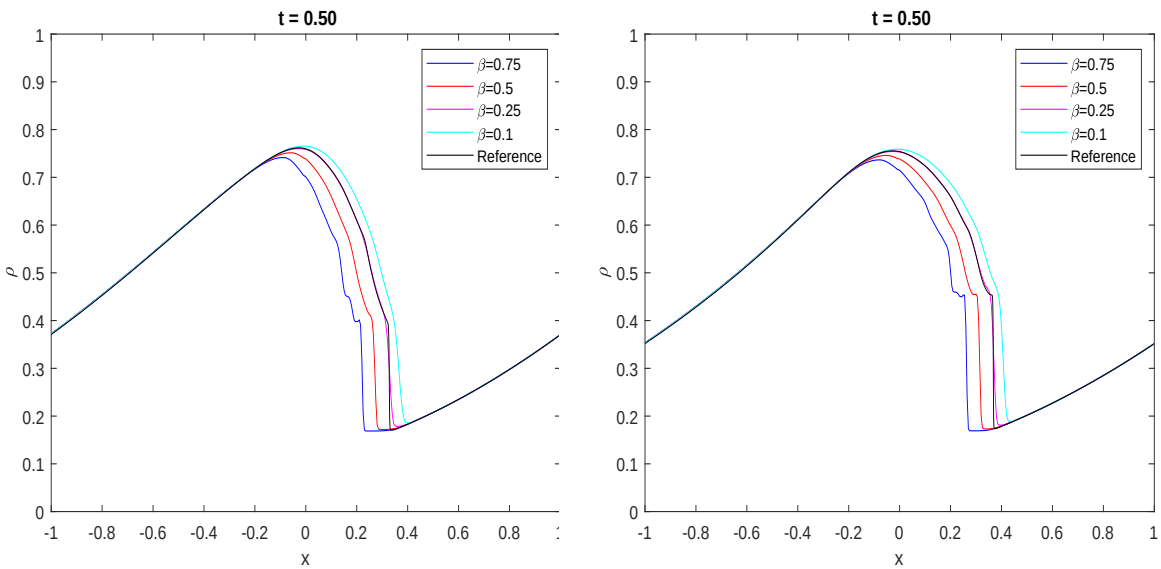

Figure 5: Solutions of (3.1), (4.2) computed by the UCS scheme using $v(\rho) = 1-\rho$ (left) and $v(\rho) = 1-\rho^2$ (right).

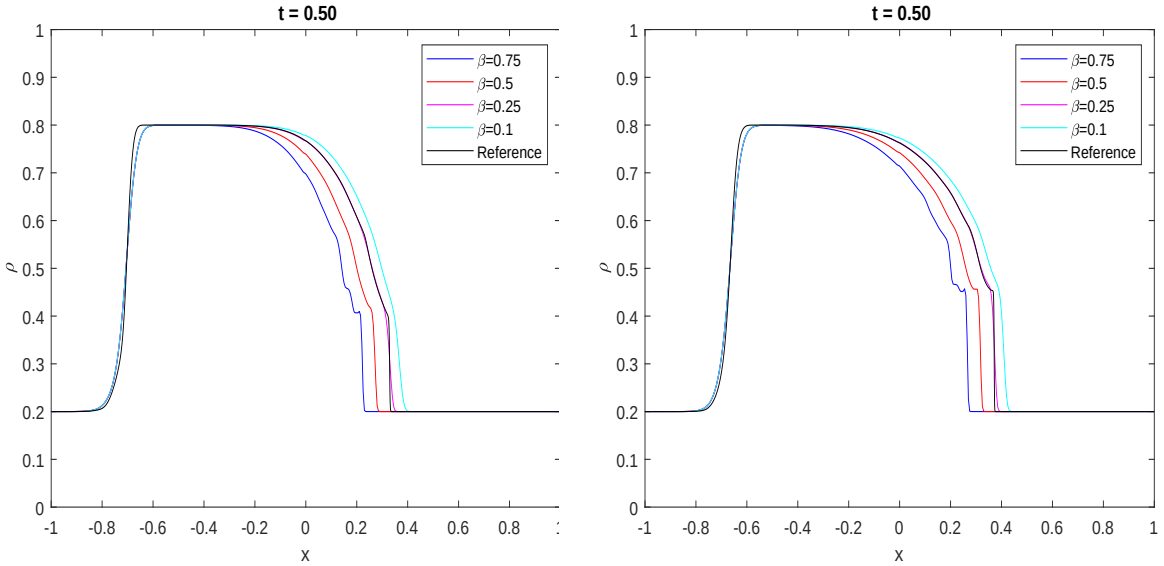

Figure 6: Solutions of (3.1), (4.1) computed by the UCS scheme using $v(\rho) = 1-\rho$ (left) and $v(\rho) = 1-\rho^2$ (right).

4.2. Comparaison to the NT original

This test aims to validate our method, by comparing some of the numerical results obtained using the UCS method with the results obtained using the original Nessyahu–Tadmor scheme. We compute the solution up to time $T = 1$, with parameters $\alpha = 0.5$, $\beta = 0.25$ and $\theta = 2$. We set $\Delta x = 0.005$ and compute the solutions with both UCS and NT schemes. The results are displayed in Figs.7 and 8. We observe that the numerical solutions obtained with the UCS scheme are in good agreement with those obtained with the NT scheme.

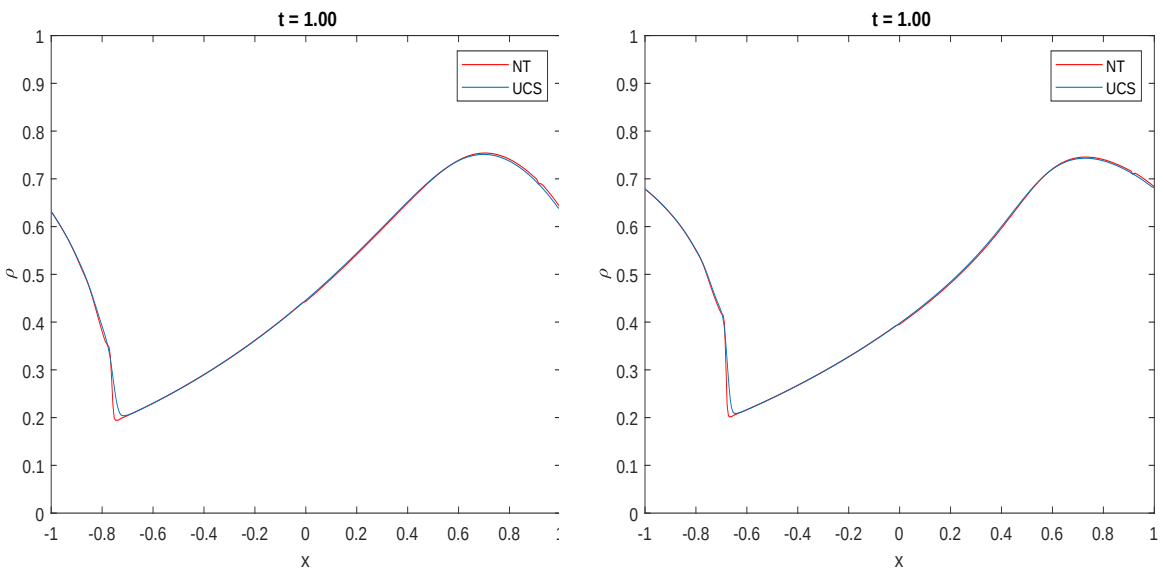

Figure 7: Comparison of numerical solutions of (3.1), (4.1) computed by the UCS scheme and the NT scheme using $v(\rho) = 1 - \rho$ (left) and $v(\rho) = 1 - \rho^2$ (right).

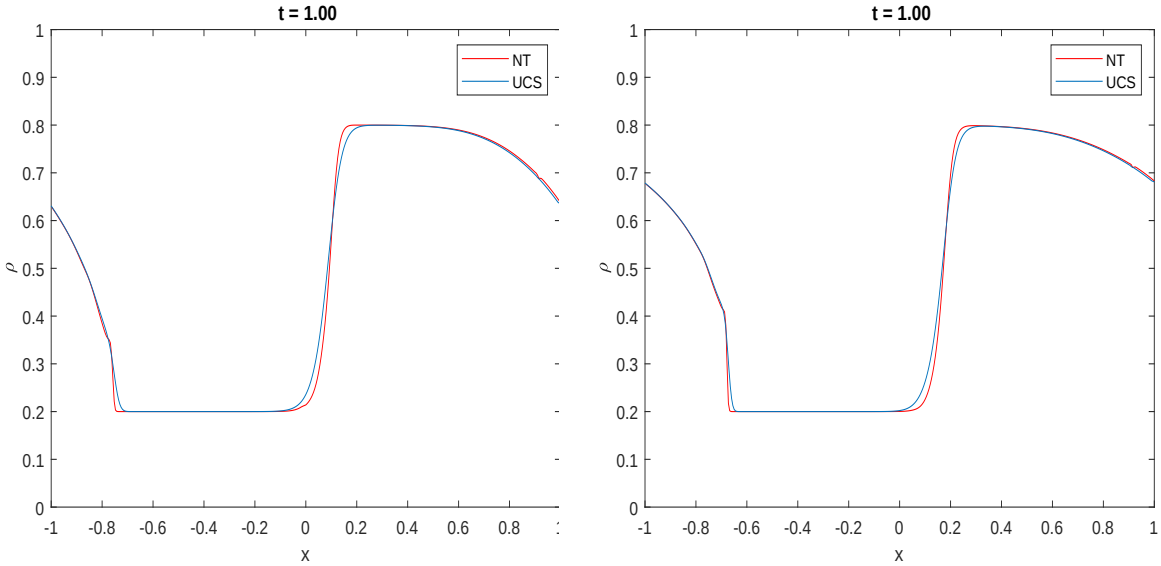

Figure 8: Comparison of numerical solutions of (3.1), (4.2) computed by the UCS scheme and the NT scheme using $v(\rho) = 1 - \rho$ (left) and $v(\rho) = 1 - \rho^2$ (right).

4.3. Accuracy test

This test aims to numerically verify if the proposed unstaggered central schemes are indeed second-order accurate; here we use a problem in the domain [-1,1] with initial conditions (4.1) and (4.2) and periodic boundary conditions.

The order of convergence is computed for different numbers of space cells as

$$\gamma(\Delta x) = \log_2 \left(\frac{e(\Delta x)}{e(\frac{\Delta x}{2})} \right),$$

where $e(\Delta x)$ denotes the L^1 error which is computed as

$$e(\Delta x) = \|\rho_{\Delta x}(T, x) - \rho_{\frac{\Delta x}{2}}(T, x)\|_{L^1}.$$

Tables 1, 2, and 3 summarize the L^1 errors and order of convergence for the UCS and NT schemes up to $T = 0.5$. With both discontinuous (4.2) and smooth initial conditions (4.1), the UCS scheme does not make significant differences in the order of convergence in comparison to the NT scheme regarding the L^1 error. It is clear that the suggested approaches maintain second-order accuracy.

Table 1: Convergence orders and L^1-errors for UCS schemes at final time $T = 0.5$ with smooth initial condition $\rho_0(x) = 0.5 + 0.4\sin(x)$ and $v(\rho) = 1 - \rho$.

	UCS							
	$\beta = 0.25$						$\beta = 0.5$	
	$\alpha = 0.5$		$\alpha = 0.25$		$\alpha = 0.75$		$\alpha = 0.5$	
N.cells	L^1error	$\gamma(\Delta x)$	L^1error	$\gamma(\Delta x)$	L^1error	$\gamma(\Delta x)$	L^1error	$\gamma(\Delta x)$
100	8.8940e-05	-	8.5607e-05	-	7.8711e-05	-	7.2917e-05	-
200	2.2358e-05	1.99	1.9985e-05	2.09	2.0174e-05	1.96	1.8986e-05	1.94
400	6.2496e-06	1.84	5.8683e-06	1.76	5.5307e-06	1.86	5.3836e-06	1.81
800	1.5936e-06	1.97	1.5718e-06	1.90	1.3539e-06	2.03	1.3374e-06	2.00
1600	4.0312e-07	1.98	4.1124e-07	1.93	3.2893e-07	2.04	3.3603e-07	1.99

Table 2: Convergence orders and L^1-errors for UCS schemes at final time $T = 0.5$ with smooth initial condition $\rho_0(x) = 0.5 + 0.4\sin(x)$ and $v(\rho) = 1 - \rho^2$.

	UCS							
	$\beta = 0.25$						$\beta = 0.5$	
	$\alpha = 0.5$		$\alpha = 0.25$		$\alpha = 0.75$		$\alpha = 0.5$	
N.cells	L^1error	$\gamma(\Delta x)$	L^1error	$\gamma(\Delta x)$	L^1error	$\gamma(\Delta x)$	L^1error	$\gamma(\Delta x)$
100	8.8649e-05	-	8.1080e-05	-	8.1560e-05	-	7.4116e-05	-
200	2.1650e-05	2.03	2.0496e-05	1.98	1.9666e-05	2.05	1.8608e-05	1.99
400	6.1587e-06	1.81	8.1040e-06	1.33	5.3171e-06	1.88	5.6372e-06	1.72
800	1.5472e-06	1.99	2.0365e-06	1.99	1.2915e-06	2.04	1.4372e-06	1.97
1600	3.5984e-07	2.10	5.2777e-07	1.94	3.0541e-07	2.08	3.6425e-07	1.98

Table 3: Convergence orders and L^1-errors for NT scheme at final time $T = 0.5$ with smooth initial condition $\rho_0(x) = 0.5 + 0.4\sin(x)$, $v(\rho) = 1 - \rho$ and $v(\rho) = 1 - \rho^2$.

	NT			
	$v(\rho) = 1 - \rho$		$v(\rho) = 1 - \rho^2$	
N.cells	L^1error	$\gamma(\Delta x)$	L^1error	$\gamma(\Delta x)$
100	8.2209e-05	-	7.1458e-05	-
200	1.7759e-05	2.21	1.8287e-05	1.96
400	4.3342e-06	2.03	4.3590e-06	2.06
800	1.0755e-06	2.01	1.0827e-06	2.00
1600	2.6678e-07	2.01	2.7443e-06	1.98

5. Conclusion

In this study, we have constructed an unstaggered central scheme for nonlocal conservation law equations. The proposed approach is based on Nessyahu-Tadmor's method, which yields numerical solutions on one grid, implicitly using ghost cells to prevent Riemann's problems at cell interfaces. The derived scheme computes a numerical solution in two phases. Moreover, since the numerical approach does not involve any characteristic field decomposition, it will significantly shorten computation times compared to methods that use approximate or exact Riemann-problem solvers. The suggested scheme is second-order accurate in both space and time due to ordering two's piecewise linear interpolants and temporal quadrature rules. For central schemes, it's common to consider a variety of limiter choices. In most cases, the generalized limiter typically produces the best results. In addition, the numerical experiments we looked at in this paper showed that $\beta = 0.25$ produces the best results by capturing discontinuities well, while our results for $\beta > 0.5$ and $\beta < 0.25$ are less satisfactory. We used both the UCS approach and the original Nessyahu and Tadmor central scheme to overcome nonlocal traffic flow concerns. Our numerical results show that the suggested method can effectively handle nonlocal traffic flow models, proving that it should be expected to realize high accuracy and ease within the central scheme family.

References

1. Aggarwal, A., Colombo, R. M., Goatin, P., *Nonlocal systems of conservation laws in several space dimensions*, SIAM J. Numer. Anal, 53 (2), 963-983, (2015).
2. Arminjon, P., Viallon, M. C. and Madrane, A., *A finite volume extension of the Lax Friedrichs and Nessyahu Tadmor schemes for conservation laws on unstructured grids*, Int. J. Comp. Fluid Dyn, 9 (1), 1-22, (1998).
3. Amorim, P., Colombo, R. and Teixeira, A., *On the numerical integration of scalar nonlocal conservation laws*, ESAIM: M2AN, 49 (1), 19-37, (2015).
4. Betancourt, F., Burger, R. and KH Karlsen, EM Tory., *On nonlocal conservation laws modelling sedimentation, Nonlinearity*, 24 (3), 855, (2011).
5. Blandin, S. and Goatin, P., *Well-posedness of a conservation law with non-local flux arising in traffic flow modeling*, Numer. Math, 132 (2), 217-241, (2017).

6. Belkadi, S. and Atounti, M., *Non oscillatory central schemes for general non-local traffic flow models*, Int. J. Appl. Math., 35 (4), 515-528 (2022).

7. Chalons, C., Goatin, P. and Villada, Luis, M., *High-Order Numerical Schemes for One-Dimensional Nonlocal Conservation Laws*, SIAM J. Sci. Comput, 40 (1), A288-A305, (2018).

8. Chiarello, F. A. and Goatin, P., *Global entropy weak solutions for general non-local traffic flow models with anisotropic kernel*, ESAIM: M2AN, 52 (1), 163-180, (2018).

9. Colombo, R. M., Garavello, M. and Lecureux-Mercier, M., *A class of nonlocal models for pedesterian traffic, ModelsMethods Appl*, 22 (4), 1150023, (2012).

10. Eymard, R., Gallouet, T. and Herbin, R., *Finite volume Method*, Handb. Numer. Anal, 7, 713-1018, (2000).

11. Friedrich, J., Kolb, O. and Gottlich, S., *A Godunov type scheme for a class of LWR traffic flow models with non-local flux*, Netw. Heterog. Media, 13 (4), 531-547, (2018).

12. Goatin, P. and Scialanga, S., *Well-posedness and finite volume approximations of the LWR traffic flow model with non-local velocity*, Netw. Heterog. Media, 11 (1),107-121, (2016).

13. Godlewski, E. and Raviart, PA., *Hyperbolic Systems of Conservation Laws*. Ellipses, (1991).

14. Jiang, G. S., Levy, D., Lin, S., T., Osher, S. and Tadmor, E., *High-resolution non-oscillatory central schemes with nonstaggered grids for hyperbolic conservation laws*, SIAM J. Numer. Anal, 35, 2147-2168, (1998).

15. Karafyllis, I., Theodosis, D. and Papageorgiou, M., *Analysis and control of a non-local PDE traffic flow model*, Int. J. Control, 95 (3), 660-678, (2022).

16. Kurganov, A. and Levy, L., *Central upwind schemes for the St. Venant system*, Math. Mod. Numer. Anal, 36, 397-425, (2002).

17. Kurganov, A. and Polizzi, A., *Non-oscillatory central schemes for a traffic flow model with Arrehenius look-ahead dynamics*, Netw. Heterog. Media, 4 (3), 431-451, (2009).

18. Li, D. and Li, T., *Shock formation in a traffic flow model with Arrhenius look-ahead dynamics*, Networks and Heterogeneous Media, 6 (4), 681-694, (2011).

19. Nessyahu, N. and Tadmor, E., *Non-oscillatory central differencing for hyperbolic conservation laws*, J. Comp. Phys, 87 (2), 408-463, (1990).

20. Sopasakis, A. and Katsoulakis, M. A., *Stochastic modeling and simulation of traffic flow: asymmetric single exclusion process with Arrhenius look-ahead dynamics*, SIAM J. Appl. Math, 66 (3), 921-944, (2006).

21. Sweby, P. K., *High resolution schemes using flux limiters for hyperbolic conservation laws*, Siam J. Num. Anal, 21, 995-1011, (1984).

22. Touma, R., *Central unstaggered schemes for one dimensional Shallow water equations*, in: Proc. Third Int. Conf. Num. App. Math. ICNAAM 2007, Corfu Greece; September (2007).

23. Touma, R., *Central unstaggered finite volume schemes for hyperbolic systems: Applications to unsteady shallow water equations*, Num. App. Math. 213 (1), 47-59, (2009).

Said Belkadi and Mohamed Atounti,
Department of Mathematics, Multidisciplinary Faculty of Nador, University Mohammed First, Oujda, Morocco.
E-mail address: s.belkadi.said@gmail.com

and

Mohamed Atounti,
Department of Mathematics, Multidisciplinary Faculty of Nador, University Mohammed First, Oujda, Morocco.
E-mail address: atounti@hotmail.fr